sciendo

ACTA CHEMICA IASI, **28_1**, 31- 46 (2020)

DOI: 10.2478/achi-2020-0003

SYNTHESIS, CRYSTAL STRUCTURE, X-RAY STUDIES, DFT OPTIMIZATION AND EVALUATION *IN VITRO* OF (*E*)-5-(BENZYLOXY)-2-{[(4-METHOXYPHENYL)IMINO]METHYL}PHENOL

Nadir Ghichi[a*], Ali Benboudiaf[a], Chawki Bensouici[b], Yacine DJebli[c], Ammari Rayenne[d], Belmanaa Radhia[d] and Hocine Merazig[a]

[a]*Unit of Research CHEMS, Chemistry Department, University of Mentouri Brothers, Constantine 1, Algeria*

[b]*Biotechnology Research Center, Constantine, Algeria*

[c]*Laboratory of Materials Chemistry, University of Mentouri Brothers, Constantine 1, Algeria*

[d]*National School Superior of Biotechnology Taoufik KHAZNADAR, Constantine, Algeria*

Abstract: The title Schiff base (Sb) compound, $C_{21}H_{19}NO_3$, was synthesized *via* the condensation reaction of 2-amino-4-methoxyphenol, with 4-(benzyloxy)-2-hydroxybenzaldehyde. The structure compound was performed by X-ray data analysis. The compound crystallises in the monoclinic $P2_1/c$ space group with a = 18.859(4)Å, b = 14.612(3)Å and c = 6.2133(12)Å. β = 97.965(8)°, V= 1695.7(6) $Å^3$ and Z = 4. In the compound the conformation about C=N imine bond is *E*. The molecule is non-planar; the central benzene ring makes dihedral angles of 6.63(9) and 63.95(9)° with the outer methoxyphenyl and phenyl rings,

* Nadir Ghichi, *e-mail:* nadirgh82@hotmail.com

respectively. In the compound there is an intramolecular O—H···N hydrogen bond forming an *S*(6) ring motif. In the crystal, molecules are predominate by C–H···π interactions. The density functional theory (DFT) optimized structure, at the B3LYP/6–311+G(*d*) level, is compared with the experimentally determined molecular structure in the solid state. The antioxidant capacity of the synthesized compound was determined by the 2,2-diphenyl-1-picrylhydrazyl hydrate (DPPH) radical scavenging, cupric reducing capacity (CUPRAC) and ferric reducing power.

***Keywords*:** Crystal structure; Schiff base; antioxidant capacity; ferric; DPPH; CUPRAC; DFT.

Introduction

The chemistry of the Schiff base compounds have been used as fine chemicals and medicinal substrates.[1] Recently, the palladium and nickel complexes revealed high activities of ethylene copolymerization.[2] They have been reported to possess pharmacological activity, including anticancer[3], antibacterial[4], and antifungal[5] properties. They are used as anion sensors[6,7], non-linear optics compounds[8], and as versatile ligands in coordination chemistry.[9,10] The common structural feature of the compound is the presence of an azomethine group linked by an η methylene bridge which can act as hydrogen-bond acceptors. In view of this interest we have synthesized the title compound (I) (Figure 1), and report herein on their crystal structure, and its DFT computational calculation. Calculations by density functional theory (DFT) on (I), carried out at the

B3LYP/6-311+G(*d*) level, are compared with the experimentally determined molecular structure in the solid state. The compound was assayed for it antioxidant activity by using *in vitro* 2,2-diphenyl-1-picrylhydrazil (DPPH) scavenging, cupric reducing capacity (CUPRAC) and ferric reducing power assay. The ^{1}H NMR and ^{13}C NMR spectra revealed the presence of an imino group (N=CH) in the region δ = 8.4 ppm and in the range 159.6-163.7 ppm respectively.

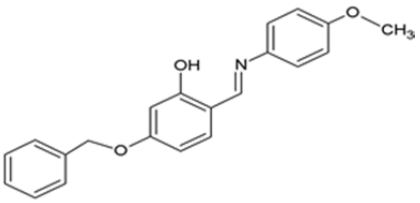

Figure 1. Molecular structure of (*E*)-5-(benzyloxy)-2-{[(4-methoxyphenyl)imino]methyl}phenol (I).

Results and discussions

Synthesis and Crystallisation

The NMR spectra were recorded on a Bruker Avance DPX 250 MHz spectrometer operating at 250 MHz for ^{1}H and at 62.5 MHz for ^{13}C nucleus.

A mixture of 2-amino-4-methoxyphenol (1 equiv.) and 4-benzyloxy-2-hydroxybenzaldehyde (1 equiv.) in ethanol (65 mL) was refluxed for 1 h and 40 min, and after that the solvent was evaporated *in vacuo*. The residue was recrystallized from ethanol, yielding green crystals of the compound on slow evaporation of the solvent. The purity of the compound was characterized by its NMR spectra. ^{1}H NMR (250 MHz, $CDCl_3$) δ: 3.8 (s, 3H; CH_3), 5.0 (s, 2H; CH_2), 6.4-7.7 (m, 12H; H-ar), 8.4 (s, 1H; N=CH), 14.0 (s, 1H; OH). ^{13}C NMR (62.5 MHz, $CDCl_3$) δ: 55.6, 70.1, 128.2, 128.7, 133.3, 136.4, 141.4, 159.6, 162.8, 163.7.

Refinement

Crystal data, data collection and structure refinement details are summarized in Table 1 and selected geometric parameters are presented in Table 2. In compound $C_{21}H_{19}NO_3$, the hydroxyl H atom was located in a difference-Fourier map and initially freely refined. In the final cycles of refinements it was positioned geometrically (O–H = 0.82Å) and refined

with *U*iso(H) = 1.5 *U*eq(O). For the compound crystallized, the C-bound H atoms were positioned geometrically (C–H = 0.93–0.97Å) and refined as riding with *U*iso(H) = 1.5 *U*eq(C).

Data collection: *APEX2*[11]; cell refinement: *SAINT*[11]; data reduction: SAINT[11]; program(s) used to solve structure: SHELXT2017[12]; program(s) used to refine structure: *SHELXL2017*[13]; molecular graphics: *SHELXTL*[14] and *Mercury*[15]; software used to prepare material for publication: *SHELXTL*[14] and *PLATON*[16].

Table 1. Structure refinement details for compound $C_{21}H_{19}NO_3$.

Chemical formula	$C_{21}H_{19}NO_3$
Formula weight	333.37
Crystal Color	green
Crystal System	Monoclinic
Space Group	$P2_1/c$
Cell parameters (Å):	
a	18.859 (4)
b	14.612 (3)
c	6.2133 (12)
Cell angles (°):	
α	90
β	97.965 (8)
γ	90
Volume ($Å^3$)*:*	1695.7(6)
T(K)	293(2)
Radiation Type	Mo*K*α
Z	4
μ/mm^{-1}	0.09
Reflections collected	17066
Data/restraints/parameters	4362/0/230
Final Rindexes [I>2σ(I)]	R1=0.057, Wr2=0.174
Goodness of Fit on F^2	0.98

Table 2. Selected geometric parameters (bond lengths [Å] and angles [°].

Bond	Length/Angle	Bond	Length/Angle
O1—C9	1.343(2)	O3—C14	1.430(2)
O2—C4	1.364(2)	N1—C1	1.419(2)
O2—C21	1.420(2)	N1—C7	1.277(2)
O3—C11	1.358(2)	O2—C4—C5	124.61(17)
C4—O2—C21	118.25(15)	N1—C7—C8	122.89(17)
C11—O3—C14	118.26(13)	O1—C9—C10	118.60(16)
C1—N1—C7	121.88(14)	O1—C9—C8	120.79(15)
N1—C1—C2	117.58(16)	O3—C11—C12	114.71(15)
N1—C1—C6	124.58(16)	O3—C11—C10	124.76(16)
O2—C4—C3	115.90(16)	O3—C14—C15	108.74(15)

Antioxidant activity

DPPH Free Radical Scavenging assay

The activity of DPPH was measured according to the protocol described by Blois[17], the principle of this method is the reduction of the DPPH, the radical form (2,2-diphenyl-1-picrylhydrazyl) with violet color to 2,2-diphenyl-1-picryl hydrazine having yellow color. DPPH absorbs at 517 nm, but when reduced by an antioxidant, its absorption decreases. Briefly, a solution of 0.4 mM of DPPH prepared in methanol and 160 μL of this solution was added to 40 μL of sample diluted in deuterated DMSO solutions of different concentrations.

30 minutes later, the absorbance was measured at 517 nm. BHT (butylated hydroxytoluene) and BHA (butylated hydroxyanisole) have been used as antioxidant standards, for the comparison of activity with the products used. The low absorbance value of the reaction of the mixture indicates higher free radical scavenging activity. The ability to trap the DPPH radical was calculated according to the following equation

$$\% \text{ Inhibition} = \frac{A_{DPPH} - A_S}{A_{DPPH}} .100\%$$

where A_{DPPH} is the absorbance of DPPH free radicals solution, A_s is the absorbance of the sample. Each experiment was performed in triplicate and average values were recorded. Results are expressed as the means ±S.D.

Cupric reducing antioxidant capacity (CUPRAC)

The cupric reducing antioxidant capacity was determined using the method of Apak[18], modified by Öztürk.[19] A solution is prepared with mixing the volumes of: 50 µL Cu (II) (10 mM), 50 µL neocuprine (7.5 mM) and 60 µL of ammonium acetate buffer solution (1 M, pH = 7.0). Different concentrations of compound were added to the initial mixture in order to make the final volume of 200 µL. After one (01) hour of incubation at room temperature, the absorbance at 450 nm was read against a blank reagent. Standard antioxidants used in this test were BHT and BHA. Results were given as absorbance and $A_{0.5}$ (µg/mL) values corresponding to the concentration indicating 0.50 absorbance intensity were assessed.

Reducing power assay

The activity of the reducing power is determined by the Oyaizu method with a slight modification. This test is considered as a direct and rapid test for measuring the reducing power of non-enzymatic antioxidants in a neutral medium.

The reductive abilities of the compound were assessed using Fe^{3+} to Fe^{2+} reductive capacity as described by Oyaizu.[20] 10 µL of each dilution of the compound was mixed with 40 µL of phosphate buffer (pH 6.6) and 50 µL of potassium ferricyanide (1 %) (1 g of $K_3Fe(CN)_6$ in 100 mL H_2O), and then the mixture was incubated at 50 °C for 20 min. 50 µL of trichloroacetic acid (TCA) (10 %), 40 µL H_2O and 10 µL ferric chloride $FeCl_3$ (0.1 %) were added to the mixture. Immediately a reading of the absorbance at 700 nm.

Structural description and crystal interactions

The X-ray data analysis structure of the (*E*)-5-(benzyloxy)-2-{[(4-methoxyphenyl)imino]methyl}phenol (I) was performed. Green crystals of compound (I) were obtained by crystallization from ethanol.

The molecular structure of compound is illustrated in Figure 1. In compound crystal, the molecular structure may be influenced by intramolecular hydrogen bond (O–H···N) (see Table 3). These hydrogen bond form *S*(6) ring motifs as shown in Figure 2. The configuration of the C=N imine bond is *E* in the compound and the C=N bond length is 1.277(2)Å for bond C7=N1. The compound is non-planar; the dihedral angle between the central benzene ring (C8–C13) and the two outer benzene rings, (C1–C6) and (C15–C20) being 6.63(9) and 63.95(9)°, respectively. Bond angles C1–N1–C7 is also near 120° [121.88 (14)°], and the imine group has a torsion angle C1–N1–C7–C8 of -178.97(16)°.

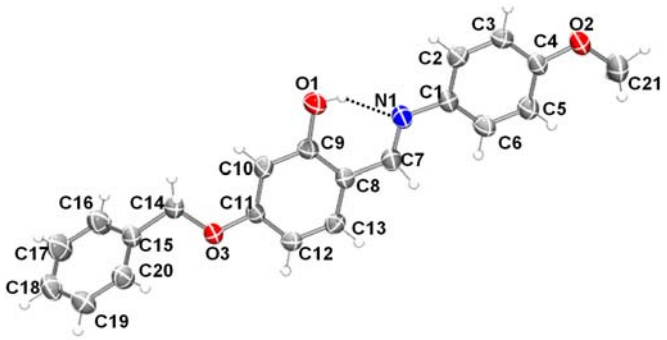

Figure 2. The asymmetric unit of (I), with the atom-numbering scheme. Displacement ellipsoids are drawn at the 50% probability level.

In the crystal structure of the compound, C–H···π interactions predominate; see Table 3.

The structure of the compound $C_{21}H_{19}NO_3$ (I), contains strong hydrogen bonds O1–H1···N1 (see Table 3). Weaker C–H···π [*Cg1, Cg2,*

Cg3] and O1–H1···N1 interactions also contribute to the packing (Figure 3). The short C3–H3···O1 contacts form a zig-zag string, along the direction of the b-axis, as shown in Figure 4. There are no other significant intermolecular contacts present in the crystal structure of compound (I).

Table 3. Hydrogen-bond geometry (lengths [Å], angles [°]).

D—H···*A*	*D*—H				H···*A*	*D*···*A*	*D*—H···*A*
O1—H1···N1	0.8200				1.8800	2.6131(19)	148.00
C5—H5···Cg1^{i}	0.9300				2.9300	3.6540(2)	136.00
C13—H13···Cg2^{i}	0.9300	2.7200	3.4141(2)	132.00			
C14—H14B···Cg3^{ii}	0.9700	2.6800	3.5030(2)	143.00			
C19—H19···Cg2^{iii}	0.9300	2.9000	3.7010(2)	146.00			

Cg1, *Cg2* and *Cg3* are the centroids of the C1–C6, C8–C13 and C15–C20 respectively.

Symmetry codes: (i) x, 3/2−y, 1/2 +z; (ii) −x, 1−y, −z;(iii) −x, 1−y, 1−z.

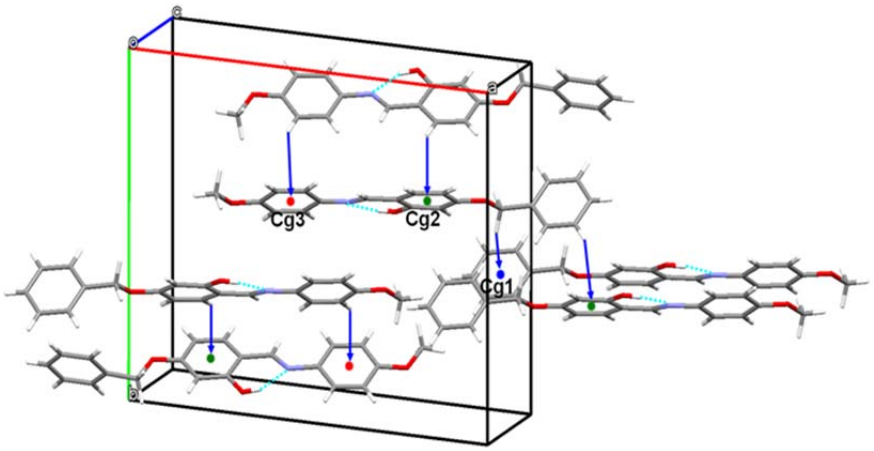

Figure 3. A view of the hydrogen bonds (dashed lines) and C–H···π interactions (blue arrows) in the crystal structure of compound (I). Centroid *Cg1* is blue, centroid *Cg2* is green and centoid *Cg3* is red (see Table 3). Only the H atoms involved in these interactions have been included.

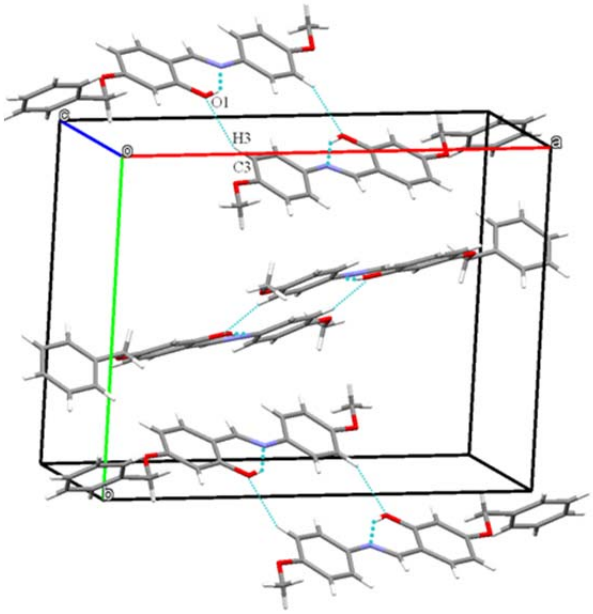

Figure 4. Zig-zag chains of molecules of (I) along the b-axis direction. Hydrogen bonds are drawn as blue dashed lines.

DFT optimized and calculation study

The DFT quantum chemical calculations were performed at the hybrid functional B3LYP[21,22], with base 6-311+G (*d*). DFT structure optimization of the title compound (Figure 5) was performed starting from the X-ray geometry and the values of geometry torsion (Table 4), distance (Table 5) and angle (Table 6) are compared with experimental values.

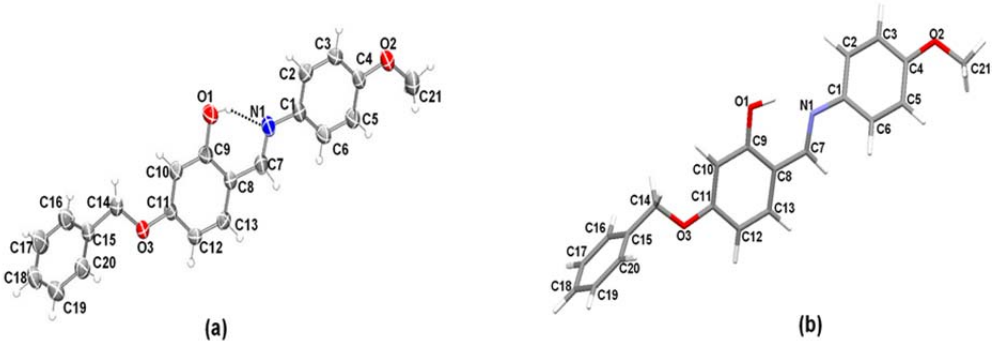

Figure 5. Comparison of the structures of (I) obtained from *(a)* the X-ray determination and *(b)* the DFT calculations.

From these results we can conclude that basis set 6-311+G (*d*) is well suited in its approach to the experimental crystallographic data. The optimized parameters, such as bond lengths and angles, are in generally good agreement (the largest bond-length deviation is less than 0.03Å) with the experimental crystallographic data (Table 5). The calculated and experimental torsion angle for N1–C1–C6–N5 is 179.27 and 179.07 (17), respectively (Table 4). The DFT study of (I) shows that the HOMO and LUMO are localized in the plane extending from the methoxybenzene ring to the phenol central ring. The electron distribution of the HOMO-1, HOMO, LUMO and the LUMO+1 energy levels are shown in (Figure 6). The HOMO and HOMO-1 molecular orbital are dominated by π-orbital density. The LUMO is mainly composed of σ density while LUMO+1 is dominated by σ electronic density and characterized in group benzyloxy. The HOMO-LUMO gap was found to be 0.1451 a.u., and the frontier molecular orbital energies, E_{HOMO} and E_{LUMO} are -5.646eV and -1.696eV, respectively.

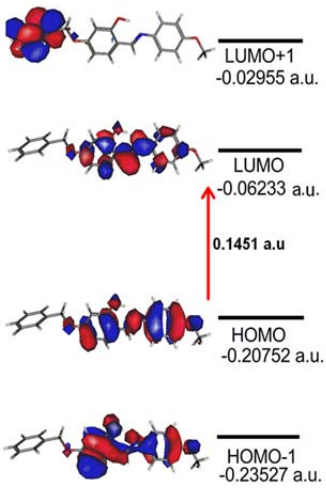

Figure 6. Electron distribution in the HOMO-1, HOMO, LUMO and LUMO+1 energy levels for (I).

Table 4. Experimental and calculated torsion lengths (°).

Parameter	X-ray	B3LYP/6-311+G(*d*)
O2—C4—C5—C6	179.74 (17)	179.99
N1—C1—C6—C5	179.07 (17)	179.27
C7—C8—C9—C10	178.99 (17)	179.98
C7—C8—C13—C12	178.59 (17)	179.96

Table 5. Experimental and calculation bond lengths (Å) for compound (I).

Parameter	X-ray	B3LYP/6-311+G(*d*)
N1—C7	1.277 (2)	1.291
O2—C4	1.364 (2)	1.365
O1—C9	1.343 (2)	1.342
O3—C14	1.430 (2)	1.438
C7—C8	1.438 (3)	1.445
O2—C21	1.420 (2)	1.419
O3—C11	1.358 (2)	1.358
C9—C10	1.383 (2)	1.399
C14—C15	1.494 (3)	1.504
C11—C12	1.392 (3)	1.409
C12—C13	1.364 (3)	1.377
C10—C11	1.383 (2)	1.393

Table 6. Experimental and calculated angles lengths (°) for compound (I).

Parameter	X-ray	B3LYP/6-311+G(*d*)
C1—N1—C7	121.88 (14)	121.38
O2—C4—C5	124.61 (17)	124.72
C7—C8—C9	121.71 (16)	121.78
C1—C2—C3	121.54 (17)	121.03
C4—O2—C21	118.25 (15)	118.58
C7—C8—C13	120.66 (17)	120.34
C11—O3—C14	118.26 (13)	118.95
O3—C14—C15	108.74 (15)	108.29
C8—C13—C12	122.18 (17)	122.06
C9—C10—C11	119.69 (17)	119.93
C17—C18—C19	119.50 (19)	119.83
O3—C14—H14A	110	109.14
O3—C14—H14B	110	109.17

The results of antioxidant activity

According to the DPPH, Cupric ion reducing antioxidant capacity and reducing power assay, the title compound (I) have a low inhibitory activity of DPPH compared to the results for butylated hydroxytoluene (BHT), butylated hydroxyanisole (BHA) and α-tocopherol (see Table 7), and the percentage (%) inhibition in cupric is large than 50 ($A_{0.5}$>50) (see Table 8), compared to the results for BHT and BHA used as a positive control.

Compound (I) showed a low reducing power (see Table 9) compared to the standards ascorbic acid, tannic acid and α-tocopherol. The lack of capacity

may be due to the absence of reducing groups.

Table 7. Inhibition of the DPPH radical by the compound (I)

Compounds	12.5 µg	25 µg	50 µg	100 µg	200 µg	400 µg	800 µg	IC_{50} µg/mL
Compound (I)	9.47±0.63	9.47±5.28	11.14±0.77	12.02±0.68	28.37±0.93	45.60±2.02	64.21±0.51	>444
BHA	76.55±0.48	79.89±0.26	81.73±0.10	84.18±0.10	87.13±0.17	89.36±0.19	90.14±0.00	6.14±0.41
BHT	49.09±0.76	72.63±2.06	88.73±0.89	94.00±0.31	94.97±0.08	95.38±0.41	95.02±0.23	12.99±0.41
α-Tocopherol	37.21±1.82	81.53±1.51	89.23±0.12	89.38±0.19	89.45±0.22	89.99±0.23	89.52±0.33	13.02±5.17

Table 8. Inhibition of CUPRAC by the compound (I).

Compounds	12.5 µg	25 µg	50 µg	100 µg	200 µg	400 µg	800 µg	$A_{0.5}$ (µg /ml)
Compound (I)	0.15±0.01	0.21±0.01	0.29±0.01	0.52±0.02	0.75±0.04	1.17±0.07	0.78±0.03	>50
BHA	1.12±0.05	1.95±0.31	3.14±0.46	3.58±0.42	3.35±0.20	3.77±0.19	3.92±0.13	5.35±0.71
BHT	1.41±0.03	2.22±0.05	2.42±0.02	2.50±0.01	2.56±0.05	2.86±0.07	3.38±0.13	8.97±3.94

Table 9. Inhibition activity of iron reducing power by the compound (I).

Compounds	3.125 µg	6.25 µg	12.5 µg	25 µg	50 µg	100 µg	200 µg	$A_{0.5}$ µg/mL
Compound (I)	0.05±0.01	0.06±0.00	0.07±0.01	0.38±0.01	0.42±0.02	0.57±0.02	0.64±0.02	>50
Ascorbic Acid	0.35±0.05	0.46±0.03	0.84±0.12	0.93±0.30	1.18±0.34	1.37±0.20	1.44±0.21	6.77±1.15
Tannic acid	0.28±0.02	0.78±0.06	1.02±0.07	1.24±0.18	0.86±0.60	1.01±0.21	1.02±0.13	5.39±0.91
α-Tocopherol	0.11±0.00	0.16±0.00	0.21±0.03	0.35±0.03	0.73±0.03	1.37±0.08	1.81±0.09	34.93±2.38

Note: In DPPH, CUPRAC antioxidant activity and ferric reducing power assay, the values expressed are the mean ±S.D. of three parallel measurements ($p<0.05$).

Conclusions

The new compound (*E*)-5-(benzyloxy)-2-{[(4-methoxyphenyl) imino]methyl}phenol was synthesized. The structure of the compound obtained was confirmed by NMR spectroscopy and by X-ray diffraction. The DFT studies optimized the structure and the evaluation *in vitro* revealed

a low inhibition, may be due to the absence of reducing groups, for example polyphenolic group.

Acknowledgements

We are grateful to the Departement of Higher Scientific Research and CHEMS Research Unit, University of Mentouri Brothers, Constantine1 for the funding of this research project and with thanks the Biotechnology Research Center, Constantine, Algeria and National School Superior of Biotechnology Taoufik KHAZNADAR, Constantine, Algeria, for your collaboration in this research.

References

1. Fun, H.K.; Quah, C.K.; Viveka, S.; Madhukumar, D.J.; Prasad, D.J. *N*-[(*E*)-4-Chloro benzylidene]-2,4-dimethylaniline. *Acta Cryst.* **2011**, *E**67***, o1932.

2. Ittel, S.D.; Johnson, L.K.; Brookhart, M. Late-Metal Catalysts for Ethylene Homo- and Copolymerization. *Chem. Rev.* **2000**, *100*, 1169–1203.

3. Villar, R.; Encio, I.; Migliaccio, M.; Gil, M.J.; Martinez-Merino, V. Synthesis and cytotoxic activity of lipophilic sulphonamide derivatives of the benzo[b]thiophene 1,1-dioxide. *Bioorg. Med. Chem.* **2004**, *12*, 963–968.

4. Pandey, S.N.; Sriram, D.; Nath, G.; De Clercg, E. Synthesis and antimicrobial activity of Schiff and Mannich bases of isatin and its derivatives with pyrimidine. *Il Farmaco*, **1999**, *54*, 624–628.

5. Singh, W.M.; Dash, B.C. Synthesis of some new schiff bases containing thiazole and oxazole nuclei and their fungicidal activity. *Pesticides*, **1988**, *22*, 33–37.

6. Dalapati, S.; Alam, M.A.; Jana, S.; Guchhait, N. Naked-eye detection of F^- and AcO^- ions by Schiff base receptor. *J. Fluorine Chem.* **2011**, *132*, 536–540.

7. Khalil, R.A.; Jalil, A.H.; Abd-Alrazzak, A.Y. Application of a Schiff base derived from sulfanilamide as an acid-base indicator. *J. Iran. Chem. Soc.* **2009**, *6*, 345–352.

8. Sun, Y.; Wang, Y.; Liu, Z.; Huang, C.; Yu, C. Structural, proton-transfer, thermodynamic and nonlinear optical studies of (E)-2-((2-hydroxyphenyl)iminiomethyl)phenolate. *Spectrochim. Acta Part A*, **2012**, *96*, 42–50.

9. Khanmohammadi, H.; Salehifard, M.; Abnosi, M.H. Synthesis, characterization, biological and thermal studies of Cu(II) complexes of salen and tetrahedrosalen ligands. *J. Iran. Chem. Soc.* **2009**, *6*, 300–309.

10. Keypour, H.; Dehghani-Firouzabadi, A.; Rezaeivala, M.; Goudarziafshar, H. Synthesis and characterization of Cd(II) macrocyclic schiff base complex with two 2-Aminoethyl pendant arms. *J. Iran. Chem. Soc.* **2010**, *7*, 820–824.

11. Bruker. *APEX2 and SAINT*. Brucker AXS Inc.; Madison, Wisconsion, USA. **2012**.

12. Sheldrick, G.M. *SHELXT* – Integrated space-group and crystal-structure determination. *Acta Cryst.* **2015**, *A**71***, 3–8.

13. Sheldrick, G.M. Crystal structure refinement with *SHELXL*. *Acta Cryst.* **2015**, *C**71***, 3–8.

14. Macrae, C.F.; Bruno, I.J.; Chisholm, J.A.; Edgington, P.R.; McCabe, P.; Pidcock, E.; Rodriguez-Monge, L.; Taylor, R.; van de Streek, J.; Wood, P.A. *Mercury CSD 2.0* – new features for the visualization and investigation of crystal structures. *J. Appl. Cryst.* **2008**, *41*, 466–470.

15. Sheldrick, G.M. A Short History of SHELX. *Acta Cryst.* **2008**, *A**64***, 112–122.

16. Spek, A.L. Structure validation in chemical crystallgraphy. *Acta Cryst.* **2009**, *D**65***, 148–155.

17. Blois, M.S. Antioxidant determinations by the use of a stable free radical. *Nature.* **1958**, *181*, 1199–1200.

18. Apak, R.; Güçlü, K.; Özyürek, M.; Karademir, S.E. Novel total antioxidant capacity index for dietary polyphenols and vitamins C and E, using their cupric ion reducing capability in the presence of neocuproine: CUPRAC Method. *J. Agric. Food Chem.* **2004**, *52*, 7970–7981.

19. Öztürk, M.; Kolat, U.; Topçu, G.; Öksüz, S.; Choudhary M.I. Antioxidant and anticholinesterase active constituents from *Micromeria*

cilicica by radical-scavenging activity-guided fractionation. *Food Chem.* **2011**, *126*, 31–38.

20. Oyaizu, M. Studies on products of browning reactions: antioxidative activities of browning reaction prepared from glucosamine. *Jap. J. Nutr*. **1986**, *44*, 307-315.

21. Becke, A.D. Density‐functional thermochemistry. III. The role of exact exchange. *J. Chem. Phys*. **1993**, *98*, 5648-5652.

22. Lee, C.; Yang, W.; Parr, R.G. Development of the Colle-Salvetti correlation-energy formula into a functional of the electron density. *Phys. Rev*. **1988**, *B37*, 785-789.